J Solid State Electrochem (2012) 16:2777–2781
DOI 10.1007/s10008-012-1708-5

ORIGINAL PAPER

Three-dimensional assembly of flower-like Au structures: the synergistic effect of macroporous structures and surface nanoarchitectures on electrocatalysis and electroanalysis

Myeounghee Hyun · Jongwon Kim

Received: 29 January 2012 / Revised: 23 February 2012 / Accepted: 26 February 2012 / Published online: 8 March 2012

Abstract We present the fabrication of a three-dimensional (3D) assembly of flower-like Au structures via the combination of 3D macroporous Au-coated microspheres and surface nanoarchitectures using electrodeposition of nanoplate Au structures. The 3D flower-like Au structures exhibit synergistically enhanced electrocatalytic activities regarding glucose oxidation and oxygen reduction compared to those of the individual 3D macroporous and nanoplate Au structures. The 3D flower-like Au structures can also be utilized as electroanalytical platforms retaining the combined advantages of both of the 3D macroporous and nanoplate Au structures.

Keywords Flower-like Au · Synergistic effect · Glucose · Electrocatalysis · Electroanalysis

Introduction

The fabrication of functional Au electrodes with hierarchical surface structures has been the subject of intensive research because these surfaces enable important applications in electrocatalysis and electroanalysis. Among the various techniques for the fabrication of functional Au surfaces, electrochemical methods provide a simple and rapid route in a controlled manner [1]. Recently, the electrochemical deposition of flower-like Au structures has received much attention because of their unique properties such as superhydrophobicity [2, 3] and surface-enhanced Raman scattering (SERS) activity [4, 5]. Flower-like Au structures also exhibit high electrochemical activity, which is useful in applications in electrocatalysis [6] and electroanalysis [7]. A schematic diagram of the flower-like Au particles electrodeposited on an electrode surface to form two-dimensional (2D) arrays is shown in Fig. 1a. The flower-like Au structure was first reported to be electrodeposited on indium tin oxide (ITO) electrodes modified with thin polypyrrole films [6]. Wang and Dong have shown that flower-like Au particles can be electrodeposited on clean ITO surfaces by controlling the electrochemical parameters [2, 5].

Additionally, three-dimensional (3D) macroporous Au structures have been prepared by the electrochemical deposition of Au on microsphere-assembled templates followed by removal of templates [8]. Bartlett et al. reported on the preparation of macroporous 3D Au films and their application in electrochemical SERS [9]. Porous 3D electrode systems exhibit unique electrochemical properties that enable useful electrochemical applications such as chemical sensors, electrocatalytic charge transfers, and biological sensing platforms [10–13]. In the present study, we intended to investigate the synergistic effect of 3D macroporous structure and 2D surface nanoarchitecture on electrocatalysis and electroanalysis.

Figure 1b represents the strategy for the fabrication of 3D porous flower-like Au (pFAu) surfaces, which consists of the formation of 3D porous Au-coated microspheres (pAuMS) followed by the electrodeposition of nanoplate Au (NpAu) on the surface of the AuMS. The 3D pFAu structures formed retain the macroporous 3D structures as well as the nanoscale surface architectures on the individual AuMS particle. The electrocatalytic activity and electroanalytical functionality of the 3D pFAu surfaces were examined

Electronic supplementary material The online version of this article (doi:10.1007/s10008-012-1708-5) contains supplementary material, which is available to authorized users.

M. Hyun · J. Kim (✉)
Department of Chemistry, Chungbuk National University, Cheongju, Chungbuk 361-763, South Korea
e-mail: jongwonkim@chungbuk.ac.kr

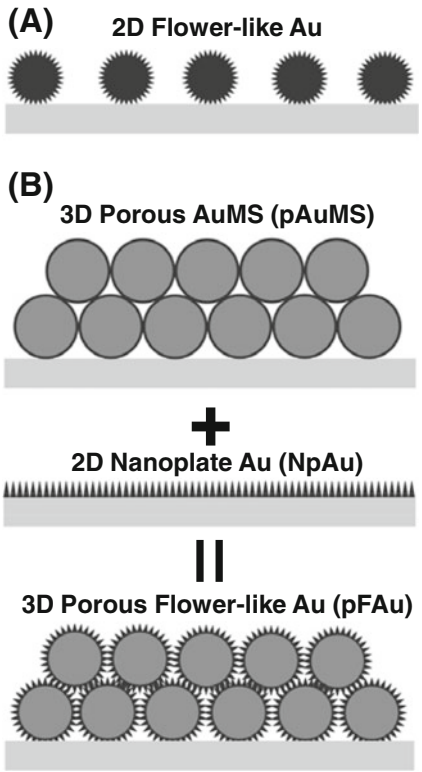

Fig. 1 Schematic diagrams of the formation of **a** 2D flower-like Au particles electrodeposited on electrodes and **b** 3D porous flower-like Au structures

and compared to those of 3D pAuMS and 2D NpAu surfaces, from which synergistic effects have been demonstrated.

Experimental

Materials and instruments

Au-coated microspheres (AuMS, an Au layer with thickness of ~50 nm was formed by the electroless plating method on a poly(methyl methacrylate) bead with a diameter of 4 μm) were purchased from Nomadien Cooperation (Seoul, Korea). $KAu(CN)_2$ (98%), Na_2CO_3 (99%), D-glucose (99.5%) and other chemicals were purchased from Sigma-Aldrich and used as received. An Au wafer with 200 nm of gold on silicon (KMAC, Korea) was confined in a Viton O-ring with an inner diameter of 2.9 mm and used as a working electrode. Electrochemical measurements were conducted using a BAS 100BW (Bioanalytical Systems, West Lafayette, USA) potentiostat. Pt wire and Ag/AgCl electrodes were used as counter and reference electrodes, respectively. All potentials are reported relative to the Ag/AgCl (3 M KCl) reference electrode. The supporting electrolytes for glucose oxidation and oxygen reduction measurements were 0.1 M phosphate buffer (pH=7) and 0.1 M H_2SO_4, respectively. Scanning electron microscopy (SEM) characterization was performed using a LEO 1530 Field Emission SEM (Carl Zeiss, Jena, Germany).

Electrode fabrication

A solution of AuMS particles dispersed in water (15 mg mL^{-1}) was sonicated before depositing onto electrode surfaces. A 10-μL portion of AuMS-dispersed solution was dropped onto electrode surfaces and dried in air to form 3D pAuMS electrodes. Electrodeposition of NpAu was performed on a flat Au electrode (for 2D NpAu) or on a 3D pAuMS (for 3D pFAu) from a solution containing 15 mM $KAu(CN)_2$ and 0.25 M Na_2CO_3. A constant deposition potential of −1.1 V was applied, and the total deposition charge was 0.04 C.

Results and discussion

Preparation of 3D porous flower-like Au structures

3D pAuMS array was first prepared by dropping AuMS particles (Fig. 2a) dispersed in water onto Au surfaces as described in our previous report [14], where we have shown that the AuMS particles deposited on Au surfaces are electrically interconnected with each other to form porous 3D assemblies. The number density of AuMS particle was estimated to be ~6×10^6 cm^{-2}. We then decorate the surface of the 3D pAuMS array with nanoplate Au structures by electrodeposition from a solution containing $Au(CN)_2^-$ [15]. A typical SEM image of the nanoplate Au structures electrodeposited on a flat Au surface is shown in Fig. 2b. The SEM image of the resulting 3D pFAu electrode is shown in Fig. 2c, where the surface of each AuMS particle has successfully been modified with nanoplate Au architectures (Fig. 2d).

The electrochemical surface area (ESA) of the Au electrode surfaces was estimated by the charge consumed by the reduction of the surface oxide layer divided by 400 μC cm^{-2} from the cyclic voltammogram of the electrodes in the Au oxide formation and dissolution region [16]. The relative ESA of the 3D pFAu surfaces with respect to bare Au surfaces was measured to be 17.0, which is equivalent to the sum of the ESAs of 2D NpAu (4.3) and 3D pAuMS (13.1) surfaces. This result indicates that the electrodeposition of NpAu is performed effectively on the surface of AuMS, and the NpAu-decorated flower-like particles are interconnected with each other to form 3D pFAu electrode surfaces.

Synergistic electrocatalysis of 3D pFAu

The electrocatalytic activity of 3D pFAu surfaces was first investigated for the oxidation of glucose, which is fairly

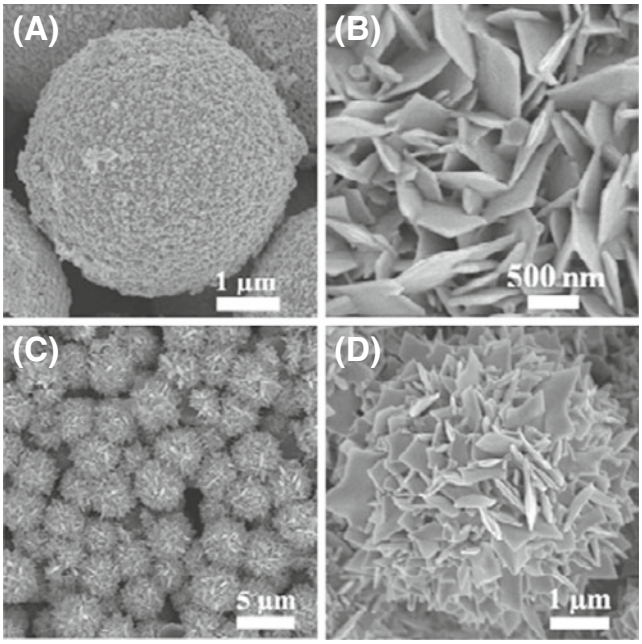

Fig. 2 SEM images of **a** an individual AuMS, **b** 2D NpAu electrodeposited on a flat Au surface, **c** a 3D pFAu electrode surface, and **d** an individual flower-like Au particle

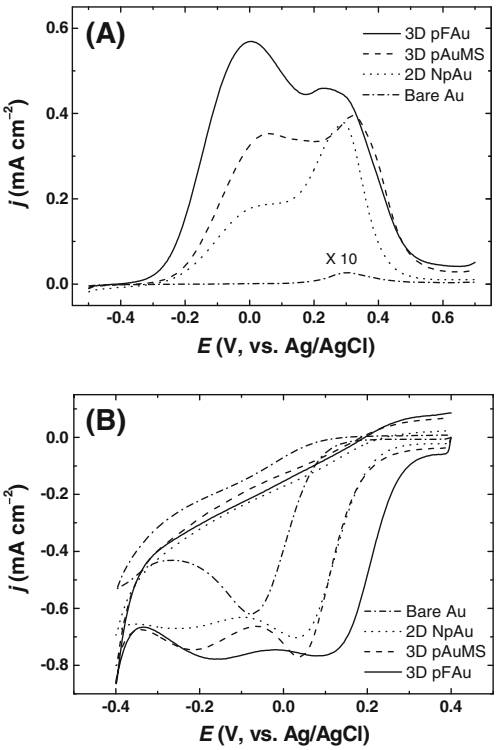

Fig. 3 **a** Anodic scans obtained in 10 mM glucose+0.1 M phosphate buffer (pH 7.0) and **b** cyclic voltammograms obtained in O_2-saturated 0.1 M H_2SO_4. Scan rate, **a** 10 mV s^{-1} and **b** 50 mV s^{-1}

sensitive to the structure of the Au surface [15, 17]. Bare Au surfaces exhibit virtually no activity in the electrooxidation of glucose; the small anodic peak at 0.3 V (dash-dotted line in Fig. 3a) is previously reported to be observed at bare Au electrodes when the surfaces are roughened [17]. It was reported that the formation of AuOH layers by chemisorption of OH^- is crucial for the electrooxidation of glucose at Au surfaces [18, 19]. As the Au electrode being roughened, Au surface domains activated for the formation of AuOH are produced, which exhibit electrochemical activity for glucose oxidation at ~0.3 V. The dotted line in Fig. 3a shows enhanced electrocatalytic activity on 2D NpAu surfaces, where the new anodic peak at 0.0 V has been ascribed to the formation of active sites on the Au nanoplate surfaces with higher surface energy, such as (110)-like Au domains [15]. The Au domains with higher surface energy enable the formation of AuOH layers at less positive potential regions, which serve as new electrocatalytically active sites for electrooxidation of glucose at ~0.0 V. The 3D pAuMS surfaces also exhibit similar electrocatalytic enhancement for glucose oxidation (dashed line in Fig. 3a), which has previously been reported for macroporous 3D inverse-opal gold film electrodes [20].

The 3D pFAu surfaces exhibit increased electrocatalytic activity, compared to the individual activities of 2D NpAu and 3D pAuMS surfaces (solid line in Fig. 3a). Here, the peak current at 0.3 V increases slightly, likely because of the increase of ESA of the 3D pFAu surfaces. On the other hand, the peak current at 0.0 V notably increases on 3D pFAu surfaces, which is not explicable simply as the increase in the ESA of 3D pFAu surfaces (Table S1 in the Electronic supplementary material (ESM)). Moreover, the current ratio between the two anodic peaks at 0.0 and 0.3 V on the 3D pFAu surfaces (1.24) is reversed compared to that of both the 2D NpAu (0.47) and 3D pAuMS (0.90) surfaces. Because the anodic currents at 0.0 V represent the unique catalytic activity in glucose oxidation, this result indicates that the electrocatalytically active sites for glucose oxidation are introduced synergistically on the 3D pFAu surface by combining the macroporous structure and surface nanoarchitecture. It should be noted that the significant catalytic effect observed on the 3D pFAu surface at 0.0 V is not affordable from each of the 2D NpAu or 3D pAuMS surfaces.

We also examined the synergistic electrocatalysis on the 3D pFAu surfaces in oxygen reduction reactions. As shown in Fig. 3b, the cathodic peak potential for oxygen reduction on 3D pFAu surfaces is observed at ~250 mV more positive potential than that on bare Au surfaces. The electrocatalytic enhancement for oxygen reduction on 3D pFAu surfaces is larger than that observed on either 2D NpAu or 3D pAuMS surfaces (both produce a 150 mV positive shift). Electrocatalysis on 2D NpAu surfaces can be ascribed to the introduction of energetically active domains such as (100) and (110) domains [15], whereas that on 3D

pAuMS surfaces can be ascribed to the porous nature (with nanometer-scale dimensions) in the vicinity of the junction of the AuMS particles [14]. X-ray diffraction (XRD) spectra of 3D pFAu and 3D pAuMS show that the XRD signals corresponding Au(100) and Au(110) at 3D pFAu increase compared to those observed at 3D pAuMS upon the formation of nanoplate Au (Fig. S1 in the ESM). Combining the 3D porosity with the surface nanoarchitectures results in unique electrocatalytic activity regarding oxygen reduction, which is not readily available on each of the 2D NpAu and 3D pAuMS surfaces. The unique electrocatalytic enhancement observed on the 3D pFAu surface for glucose oxidation and oxygen reduction demonstrates that a synergistic effect on electrocatalysis is obtained by combining the 2D NpAp and 3D pAuMS structures.

Synergistic electroanalysis of 3D pFAu

The electrochemical detection of glucose is important in non-enzymatic glucose sensors [21]. There are two main problems to be resolved in the practical electrochemical sensing of glucose in physiological media; (1) overcoming the deactivation of electrode activity caused by the presence of Cl^- ions and (2) discriminating the interference from the oxidation of ascorbic acid (AA). In our previous report, the 2D NpAu surface was shown to be relatively resistant to the surface deactivation by Cl^- compared to other Au nanostructures [15]. Figure 4a shows that the anodic current level on 2D NpAu surfaces for glucose oxidation at 0.3 V in the presence of 10 mM of Cl^- is ca. 60% of that measured in the absence of Cl^-, whereas there is a great decrease in anodic current levels on 3D pAuMS surfaces (~40%). The 3D pFAu surfaces retain a relatively high current level at 0.3 V for glucose oxidation in the presence of Cl^- (as compared to that observed in the absence of Cl^-, ~85%). In neutral phosphate buffer solutions, glucose electrooxidation current is known to decrease proportionally to the concentration Cl^- due to the blocking active sites for AuOH formation by Cl^-, and stronger effect is observed at less positive potentials [22]. Figure 4a shows that the glucose oxidation at 3D pFAu surfaces at 0.0 V quickly vanishes in the presence of Cl^-, whereas the anodic currents at 0.3 V is maintained at relatively high level when compared to the anodic scan in the absence of Cl^- shown in Fig. 3a. Therefore, the 3D pFAu surface is more resistive to the deactivation by Cl^- than either 2D NpAu or 3D pAuMS surfaces. The deactivation of electrode activity for glucose oxidation is more significant in the presence of 50 mM of Cl^- on the 2D NpAu and 3D pAuMS surfaces, whereas the 3D pFAu surface maintains relatively high current levels in the presence of 50 mM of Cl^- (Fig. 4b).

It is well known that porous structures can be effectively utilized to remove the interference of AA oxidation on the electrochemical detection of glucose owing to the different rate of electrode kinetics between AA and glucose [23]. Redox species with slow electrode kinetics (glucose) fully utilize the ESA of porous electrode surfaces, whereas those with fast electron transfer kinetics (AA) retain thick diffusion layers, thus the redox currents are proportional to the apparent geometric area. We have shown that the porous nature of 3D pAuMS structures is efficient to remove the interference from AA on the electrochemical detection of glucose [14]. Because the 3D pFAu surfaces also possess

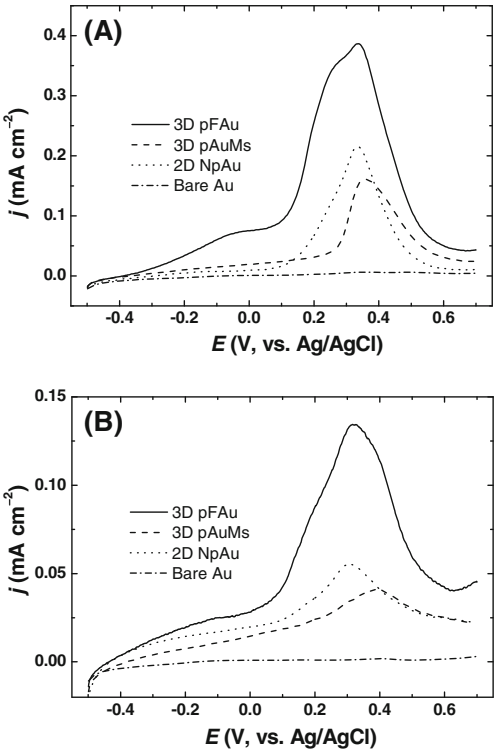

Fig. 4 Anodic scans obtained in 10 mM glucose+0.1 M phosphate buffer (pH 7.0) in the presence of **a** 10 mM Cl^- and **b** 50 mM Cl^-. Scan rate, 10 mV s^{-1}

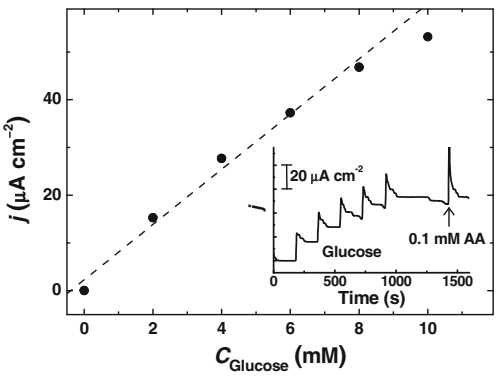

Fig. 5 Calibration plot obtained from amperometric responses at 0.3 V (*inset*) from 3D pFAu surfaces in the presence of 50 mM Cl^-

porous structures, the interference from AA can be readily eliminated during the amperometric detection of glucose (inset of Fig. 5). The concentration of AA (0.1 mM) was chosen based on the normal physiological level of AA, which is much lower than that of glucose (3~8 mM) [18, 23]. It should be noted that the porous nature of 3D pFAu surfaces enables the discrimination between glucose and AA oxidation, which cannot be achievable through the conventional 2D planar nanoflower arrays. In addition to their sustained electrochemical activity for glucose oxidation in the presence Cl^-, the 3D pFAu surfaces provide a calibration plot for glucose detection in the presence of 50 mM Cl^- without being interfered by AA (Fig. 5). A deviation from linear response at higher concentration of glucose was also reported in other nanostructured Au surfaces for glucose detection in the presence of Cl^- [24–26], probably due to the deactivation of electrode activity at elongated measurements. The sensitivity was measured to be 5.8 μM mM^{-1} cm^{-2}, which is comparable with those of other nanostructured Au surfaces, but somewhat lower than those of nanoporous Au electrodes with very high ESA [25]. The improvement of the electrode system suggested in this work for practical electrochemical glucose sensing will be the focus of the future work.

Conclusions

We have prepared a 3D assembly of flower-like Au (pFAu) structures using the electrodeposition of 2D nanoplate Au (NpAu) structures on 3D macroporous Au-coated microspheres (pAuMS). The electrocatalytic activity of 3D pFAu structures regarding glucose oxidation and oxygen reduction are synergistically enhanced compared to those of the individual 2D NpAu and 3D pAuMS structures. The 3D pFAu structures can also serve as active electroanalytical platforms, yielding the combined advantages of both of the 2D NpAu and 3D AuMS structures. We expect the strategy presented in this study to induce a synergistic effect of micro- and nanoarchitecture, which will allow the fabrication of highly functional surfaces for use in electrocatalytic and electroanalytical applications.

Acknowledgments This work was supported by the Korea Research Foundation Grant funded by the Korean Government (MOEHRD, Basic Research Promotion Fund; KRF-2008-331-C00187) and by the Basic Science Research Program through the National Research Foundation of Korea (NRF) funded by the Ministry of Education, Science, and Technology (2010-0004126).

References

1. Plowman B, Ippolito SJ, Bansal V, Sabri YM, O'Mullane AP, Bhargava SK (2009) Chem Commun: 5039–5041
2. Wang L, Guo SJ, Hu XG, Dong SJ (2008) Electrochem Commun 10:95–99
3. Zhang H, Xu JJ, Chen HY (2008) J Phys Chem C 112:13886–13892
4. Ye W, Wang D, Zhang H, Zhou F, Liu W (2010) Electrochim Acta 55:2004–2009
5. Guo S, Wang L, Wang E (2007) Chem Commun: 3163–3165
6. Li Y, Shi GQ (2005) J Phys Chem B 109:23787–23793
7. Das AK, Raj CR (2010) J Electroanal Chem 638:189–194
8. Bartlett PN, Baumberg JJ, Coyle S, Abdelsalam ME (2004) Faraday Discuss 125:117–132
9. Abdelsalam ME, Bartlett PN, Baumberg JJ, Cintra S, Kelf TA, Russell AE (2005) Electrochem Commun 7:740–744
10. Chen XJ, Wang YY, Zhou JJ, Yan W, Li XH, Zhu JJ (2008) Anal Chem 80:2133–2140
11. Wang CH, Yang C, Song YY, Gao W, Xia XH (2005) Adv Funct Mater 15:1267–1275
12. Walcarius A, Kuhn A (2008) Trac Trends Anal Chem 27:593–603
13. Walcarius A (2010) Anal Bioanal Chem 396:261–272
14. Hyun M, Choi S, Kim J (2010) Anal Sci 26:129–132
15. Seo B, Choi S, Kim J (2011) ACS Appl Mater Interfaces 3:441–446
16. Trasatti S, Petrii OA (1991) Pure Appl Chem 63:711–734
17. Cho S, Shin H, Kang C (2006) Electrochim Acta 51:3781–3786
18. Toghill KE, Compton RG (2010) Int J Electrochem Sci 5:1246–1301
19. Hsiao MW, Adzic RR, Yeager EB (1992) Electrochim Acta 37:357–363
20. Bai Y, Yang WW, Sun Y, Sun CQ (2008) Sens Actuators B 134:471–476
21. Park S, Boo H, Chung TD (2006) Anal Chim Acta 556:46–57
22. Vassilyev YB, Khazova OA, Nikolaeva NN (1985) J Electroanal Chem 196:127–144
23. Park S, Chung TD, Kim HC (2003) Anal Chem 75:3046–3049
24. Li Y, Song YY, Yang C, Xia XH (2007) Electrochem Commun 9:981–988
25. Xia Y, Huang W, Zheng JF, Niu ZJ, Li ZL (2011) Biosens Bioelectron 26:3555–3561
26. Seo B, Kim J (2010) Electroanalysis 22:939–945